

Macrophage Membrane-Coated Nanoparticles Alleviate Hepatic Ischemia-Reperfusion Injury Caused by Orthotopic Liver Transplantation by Neutralizing Endotoxin

This article was published in the following Dove Press journal:
International Journal of Nanomedicine

Zhibing Ou^{1,*}
Hua Zhong^{2,*}
Liang Zhang^{2,3}
Minghua Deng²
Wenfeng Zhang²
Jingyuan Wang²
Huaguo Feng²
Jianping Gong²
Chunmu Miao²
Zhujun Yi²

¹Department of Hepatobiliary Surgery, Chenzhou No.1 People's Hospital, Chenzhou, Hunan 410000, People's Republic of China; ²Department of Hepatobiliary Surgery, The Second Affiliated Hospital of Chongqing Medical University, Chongqing 40000, People's Republic of China; ³Institute of Ultrasound Imaging, Department of Ultrasound, The Second Affiliated Hospital of Chongqing Medical University, Chongqing 40000, People's Republic of China

*These authors contributed equally to this work

Purpose: To investigate the effect and mechanism of macrophage membrane-coated nanoparticles (M-NPs) on hepatic ischemia-reperfusion injury (I/R) caused by orthotopic liver transplantation. In addition, the advantages of TLR4⁺/M-NPs compared to M-NPs are discussed.

Materials and Methods: We prepared biomimetic M-NPs and identified their characteristics. M-NPs were injected into an SD rat model of orthotopic liver transplantation, and the anti-inflammatory and anti-I/R activities of M-NPs were studied in vivo and in vitro. In addition, we overexpressed macrophage membrane Toll-like receptor 4 (TLR4) in vitro and prepared TLR4⁺/M-NPs. Then, we assessed the characteristics and advantages of TLR4⁺/M-NPs.

Results: The M-NPs neutralized endotoxin, inhibited the overactivation of Kupffer cells (KCs) and suppressed the secretion of inflammatory factors by inhibiting the endotoxin-mediated TLR4/MyD88/IRAK1/NF-κB signaling pathway. In an orthotopic liver transplantation model in SD rats, M-NPs showed significant therapeutic efficacy by neutralizing endotoxin and suppressing the secretion of inflammatory factors. Moreover, overexpression of TLR4 on the macrophage membrane by using a TLR4⁺-plasmid in vitro effectively reduced the amount of M-NPs needed to neutralize an equivalent dose of endotoxin, reducing the potential risks of NP overuse.

Conclusion: This study indicates that M-NPs can effectively alleviate I/R induced by liver transplantation.

Keywords: biomimetic nanoparticle, endotoxin, Kupffer cell, liver transplantation, ischemia reperfusion injury

Introduction

Liver transplantation is the most effective method to treat end-stage liver diseases, but it still faces many challenges, such as the insufficiency of liver sources, immune rejection of the donor liver by the recipient, and hepatic ischemia-reperfusion injury (I/R) after liver transplantation.^{1,2} Studies have confirmed that liver transplantation I/R is closely related to the susceptibility of Kupffer cells (KCs) in the liver to endotoxin during reperfusion, which primarily occurs because liver transplantation recipients often have different degrees of endotoxemia before the operation, and portal vein occlusion during liver transplantation also causes intestinal endotoxin

Correspondence: Zhujun Yi; Chunmu Miao
Department of Hepatobiliary Surgery, The Second Affiliated Hospital of Chongqing Medical University, Chongqing 40000, People's Republic of China
Tel +86-15803630430
Email 792937539@qq.com;
luckmum@163.com

accumulation in the portal vein.^{3,4} In addition, KCs are especially sensitive to endotoxins due to the interruption of portal vein blood.⁴ The above factors lead to the activation of KCs by a large amount of endotoxin during liver transplantation, which activates the inflammatory pathway, thus promoting the release of inflammatory factors such as tumor necrosis factor- α (TNF- α) and interleukin-6 (IL-6) that induce hepatic I/RI.^{3,5} The specific molecular mechanism may be related to endotoxin recognition by Toll-like receptor 4 (TLR4) on KC membranes, which activates the myeloid differentiation factor 88 (MyD88)/interleukin receptor associated kinase 1 (IRAK1)/NF- κ B inflammatory pathway and promotes the release of inflammatory factors.^{3,5} Endotoxin is the lipopolysaccharide (LPS) component of the Gram-negative bacteria cell wall.⁶ If the concentration of endotoxin in the blood in liver transplantation can be effectively reduced, the overactivation of KCs will be effectively suppressed, thus inhibiting hepatic I/RI after liver transplantation.⁵⁻⁷

Recently, cell membrane-coated nanoparticles have emerged as a promising therapeutic platform.⁸ The cell membrane-coated nanoparticles prepared by this method not only have the transfer function of nanoparticles but also the biological function of the cell membrane, and targeted treatment of damaged areas is possible through the transfer of nanoparticles.⁹ Researchers coated nanomaterials with the membranes of neutrophils to treat the synovitis of joints and reduce joint damage caused by joint inflammation.¹⁰ Nanoparticles prepared by this method not only have the neutrophil membrane function of neutralizing proinflammatory factors but are also capable of targeted infiltration into the damaged areas, thus achieving targeted treatment.¹⁰ Furthermore, nanoparticles coated with human platelet membranes have immunomodulatory functions and adhesion antigens associated with platelets.¹¹ Moreover, nanoparticles coated with red blood cell membrane have the ability to absorb membrane-damaging toxins and divert them away from their cellular targets.¹²

KCs are macrophages located in the hepatic sinusoid and account for 80–90% of the total macrophages in the body.¹³ Many studies have confirmed that PLGA nanoparticles injected into the body are mainly distributed in the liver.¹⁴ Hepatic I/RI in liver transplantation is mainly caused by a large amount of endotoxin, which activates inflammatory pathways and promotes the release of inflammatory factors by binding to TLR4 on KC membranes.⁵ TLR4 is widely present on various macrophage membranes.^{5,15} Therefore,

we aimed to synthesize macrophage membrane-coated nanoparticles (M-NPs) with macrophage membrane functions (enriched in TLR4) and inject the M-NPs into the body. Because M-NPs are mainly localized to the liver, endotoxin can bind to TLR4 on M-NPs, thus leading to the adsorption of a large amount of endotoxin. Reducing the endotoxin-induced activation of KCs, inhibiting the release of inflammatory factors and ultimately alleviating hepatic I/RI after liver transplantation would improve the prognosis of liver transplantation recipients. Here, we established an orthotopic liver transplantation model in SD rats and explored the effect and molecular mechanism of M-NPs on hepatic I/RI in rat orthotopic liver transplantation by synthesizing M-NPs and injecting them into rats through the tail vein.

Materials and Methods

Cell Culture

The RAW264.7 mouse macrophage line was purchased from American Type Culture Collection (ATCC) and cultured in medium (DMEM, HyClone) with 10% FBS (PAN) and 1% penicillin–streptomycin (Beyotime) at 37 °C in a 5% CO₂ environment.

Macrophage Membrane Derivation

Plasma membranes of RAW264.7 macrophages were harvested following a previously published protocol.^{8,16} Briefly, RAW264.7 macrophages in a good growth state were washed with PBS (HyClone) three times and then collected (centrifugation at 800 \times g for 5 min). The cells were then suspended in a hypotonic solution containing 30 mM Tris-HCl, 225 mM d-mannitol, 75 mM sucrose and 0.2 mM EGTA (all reagents purchased from Sigma). The cells were then disrupted with 20 passes using a dounce homogenizer. After this step, all of the cells were ruptured. Then, the suspension solution was centrifuged at 20,000 \times g for 25 min at 4 °C. The precipitate was discarded, and the supernatant was transferred to a new tube and centrifuged again at 100,000 \times g for 35 min at 4 °C. After centrifugation, the supernatant was discarded, and the pellet contained the macrophage membranes. The obtained macrophage membranes were stored for a short time at –80°C. The membrane protein content was quantified with a BCA assay (Beyotime). In addition, we also extracted whole protein and nuclear protein from the cells with appropriate protein extraction kits (Sangon Biotech) and quantified the protein extracts with a BCA assay (Beyotime).

Macrophage Membrane-Coated Nanoparticle Preparation and Characterization

First, 150~180 nm polymeric cores were prepared using 0.67 dL/g carboxyl-terminated 50:50 poly (lactic-co-glycolic) acid (PLGA) (LACTEL Absorbable Polymers) by nanoprecipitation. The PLGA polymer was dissolved in acetone at a concentration of 10 mg/mL. Then, 1 mL of the solution was diluted with 3 mL of water. For fluorescently labeled PLGA cores, 1,1-dioctadecyl-3,3,3',3'-tetramethylindocarbocyanine perchlorate (DiR, excitation/emission = 748 nm/780 nm; Ye Sen) was loaded into the polymeric cores at 0.1 wt %. The nanoparticle solution was then stirred in open air for 2 h to remove the organic solvent. Then, the extracted macrophage membranes with the PLGA cores were mixed in a mass ratio of 1:2 and the mixed solution was repeatedly extruded through a liposome extruder (Sigma) to obtain macrophage membrane-coated nanoparticles (M-NPs). The macrophage membrane coating was detected by transmission electron microscopy (TEM) and the size of NPs and M-NPs were measured by dynamic light scattering (DLS).

Since macrophages contain cell membranes and nuclear membranes, we further detected the expression of related marker proteins on the M-NPs. Antibodies against F4/80 (ab6640, Abcam), TLR4 (ab13556, Abcam), CD206 (ab64693, Abcam) and CD11c (ab52632, Abcam) was used to detect markers of the macrophage membrane. The antibody against LanminA/C was used to detect a marker of the cell nucleus. Western blotting was used to detect the protein expression in cell homogenates (Hom), membranes (Mem), nuclei (Nuc) and M-NPs. Briefly, proteins were extracted with a protein extraction kit (KeyGene), and the protein concentration was detected with a BCA kit (Beyotime) in each group. The protein and 5 × loading buffer (Beyotime) were mixed in a volume ratio of 4:1 and boiled in water for 10 min. Then, 30 µg of each protein sample was separated by electrophoresis (Bio-Rad) at 120 V for approximately 2 h. The proteins were transferred to a PVDF membrane at 250 mA. The membranes were blocked with 5% milk in TBS/Tween 20 (0.5%) (TBST) for 1 h at room temperature and then incubated with primary antibody (1:1000, Abcam) overnight at 4 °C. After washing three times with TBST and adding HRP-conjugated secondary antibody (1:10,000, CST) for 1 h at room temperature, the membranes were washed three times with TBST and developed with a freshly prepared luminol-based developing solution.

Plasmid Transfection of RAW264.7 Macrophages

Plasmids with green fluorescent genes that overexpressed and silenced TLR4 were purchased from Sangon Biotech. Plasmid transfection of the RAW264.7 macrophages was performed according to a previously published protocol.¹⁷ Briefly, the plasmids was transformed into *Escherichia coli*, and *Escherichia coli* containing a large number of plasmids was obtained through expanded culture. Then, the plasmids were extracted from the genomic DNA of the *Escherichia coli*. Finally, plasmid DNA was transfected into the macrophages. A total of 3 µL of purified plasmid DNA was dissolved in 250 µL of serum-free and penicillin-streptomycin-free DMEM, mixed gently, and incubated at room temperature for 5 min. Then, 10 µL of liposome was dissolved in 250 µL of serum-free and penicillin-streptomycin-free DMEM, mixed gently, and incubated at room temperature for 5 min. The prepared DNA was mixed with liposomes and incubated at room temperature for 20 min to obtain wrapped liposomes/DNA. The liposomes were added to RAW264.7 macrophages in a good growth state for continuous culture for 10 h, and then the liquid was changed, and DMEM with 10% FBS was added for further culture for 48 h. The fluorescence expression of the cells was observed under an inverted microscope. Western blotting and reverse transcription-quantitative PCR (qRT-PCR) was used to detect the protein and nucleic acid expression of TLR4 in cells, respectively. qRT-PCR was performed as previously described.¹⁸ Primers for qRT-PCR were obtained from Sangon Biotech. The primers used were as follows: TLR4 forward 5'-ATTTCGCTTCCTGGTCT-3' and reverse 5'-GTCATCCCACTTCCTTCCT-3'; and GAPDH forward 5'-CACCACTCCTCCACCTTTG-3' and reverse 5'-CCACCACCCTGTTGCTGTAG-3'.

M-NP Neutralization of LPS in vitro

RAW264.7 macrophages were used to explore the effect of M-NPs on LPS-mediated cell activation and its molecular mechanism. Cells were cultured in medium (DMEM) (HyClone) with 10% FBS (PAN) and 1% penicillin-streptomycin (Beyotime) at 37 °C in a 5% CO₂ environment. The cells were divided into six groups with 1 × 10⁶ cells in each group. Each group was stimulated with 150 ng/mL LPS (Sigma), and different concentrations of M-NPs (0, 0.5, 1.0, 2.0, 3.0 and 5.0 mg/mL) were added to each group of LPS-stimulated macrophages. Twenty-four hours later, Western blotting was used to detect the protein

expression of MyD88, IRAK1, phosphorylation NF- κ B (p-p65) and p65. ELISA was used to detect the remaining LPS and the inflammatory factors TNF- α and IL-6 in the supernatant.

Cell viability was also used to evaluate LPS neutralization by M-NPs. Briefly, 5×10^3 cells were seeded in each well of a 96-well plate in 100 μ L of medium and cultured for 24 h. Then, 10 μ L of Cell Counting Kit-8 (CCK8, Beyotime) was added to each well, and the cells were incubated at 37 °C for 1 h. The absorbance of each well was detected at 450 nm using an enzyme reader.

To study whether in vitro overexpression of TLR4 on the macrophage membrane reduced the usage of M-NPs, thus reducing the toxic effect of M-NPs on macrophages, TLR4 on the cell membrane of RAW264.7 macrophages was effectively silenced or overexpressed by plasmid transfection. TLR4⁺/M-NPs and TLR4⁻/M-NPs were successfully synthesized by previous methods. The cells were divided into six groups, with 1×10^6 cells in each group, and cultured in 6 cm petri dishes. The control group was not treated. The LPS group was treated with 150 ng/mL LPS for 24 h. The M-NP group was treated with 1 mg/mL M-NPs for 24 h. The LPS + M-NP group, LPS + TLR4⁺/M-NP group and LPS + TLR4⁻/M-NP groups were treated with 150 ng/mL LPS for 24 h, and the corresponding M-NPs at a concentration of 1 mg/mL were added at the same time. Twenty-four hours later, Western blotting was used to detect the protein expression of MyD88, IRAK1, p-p65 and p65. ELISA was used to detect the remaining LPS and the inflammatory factors TNF- α and IL-6 in the supernatant.

Animal Care and Liver Transplantation

All male SD rats were purchased from the Experimental Animal Center of Chongqing Medical University and were housed in a specific pathogen-free (SPF) animal facility at the Experimental Animal Center of Chongqing Medical University. The animals were maintained under the guidelines of the Animal Care and Use Committee of Chongqing Medical University and this study was approved by the Research Ethics Committee of Chongqing Medical University (2019–107).

The rats were anesthetized with 5% chloral hydrate. 15 mg/kg NPs or M-NPs with the fluorescent probe (DiR, excitation/emission = 748 nm/780 nm; Ye Sen) were administered to the rats by tail vein injection for 24 h. The distribution of the M-NPs or NPs by was determined by detecting the fluorescence distribution in the rats.

Liver transplantation of SD rats ([Supporting Information Figures](#))

Procedures for liver transplantation of SD rats followed a previously published protocol.^{19,20} In brief, rat liver transplantation mainly includes two steps: donor liver preparation and recipient preparation. (1) To prepare the donor liver: SD rats weighing 200 g were selected for preoperative fasting and drinking for 24 h. The donor rats were administered 40 mg/kg sodium pentobarbital by intramuscular injection, the abdominal hair was shaved off after anesthesia, and the abdomen was disinfected with iodophor. A cross incision was made in the abdomen to expose the inferior hepatic vena cava and the right lumbar vein. Heparin was injected through the lumbar vein. The lower end of the abdominal aorta was freed and exposed for later use. The inferior hepatic vena cava, the right renal vein and the right adrenal vein were freed. The adrenal vein and the right renal vein were ligated and severed. The left adrenal gland was exposed and the fascia was torn open with microscopic forceps. The abdominal aorta was freed and clamped with a blood vessel clamp. Then, the lower segment of the abdominal aorta was perfused with cold physiological saline and residual blood in the liver was fully perfused and removed. The portal vein and inferior vena cava of the liver were freed and cut off. Finally, the superior and inferior vena cava of the liver were cut and placed into a sterile petri dish filled with 4°C Ringer's solution. The inferior vena cava and portal vein were catheterized. The superior and inferior vena cava of the liver was equipped with a needle and thread for standby. (2) To prepare the recipients, SD rats weighing 200 g were selected for preoperative fasting and drinking. The donors were administered 40 mg/kg sodium pentobarbital by intramuscular injection, the abdominal hair was shaved off after anesthesia, and the rats were disinfected with iodophor. The abdominal cavity was opened through a median abdominal incision, and the left inferior phrenic vein was ligated and severed. The remaining liver lobes were freed, the bile duct and portal vein were exposed, and the ligate bile duct it was severed. The hepatic artery was ligated and freed, and the portal vein was fully freed. The area of inferior hepatic vena cava and right renal vein were exposed, the inferior hepatic vena cava, right renal vein and right adrenal vein were freed, and the right adrenal vein was freed and disconnected. The esophageal vein was ligated and disconnected. Arterial clamps were applied to the inferior vena cava and portal vein of the liver. Starting from the nonhepatic phase, 2 mL of normal saline was

injected through the portal vein to enable blood in the liver to enter the systemic circulation. The superior and inferior vena cava of the liver were clamped above the diaphragm ring, and each blood vessel was cut off and removed from the liver. Gauze was soaked and used to cover the abdominal cavity, the donor liver was laid flat on the gauze, and the anterior and posterior walls of the upper and lower liver cavities were sutured by a continuous suture method to prevent residual lacunae. The donor liver side catheter was inserted into the recipient inferior hepatic cavity and portal vein and ligated, and the arterial clamp and vascular clamp were opened to restore blood flow. When the liver was hyperemic and ruddy, the nonhepatic phase ended, ensuring that the nonhepatic phase occurred within 30 min. Mesentery was repositioned with wet cotton swabs, and the abdominal wall was disinfected and sutured, completing the operation, after which we waited for the recipient rats to wake up.

M-NP Neutralization of LPS in vivo

The efficacy of M-NPs in neutralizing LPS was first evaluated with an SD rat liver transplantation model. Thirty rats were randomly divided into six groups: Blank group (Blank, $n = 5$); Liver transplantation group (Control, $n = 5$); Liver transplantation + NPs group (NPs, $n = 5$); Liver transplantation + M-NPs group (M-NPs, $n = 5$); Liver transplantation + TLR4⁺/M-NPs group (TLR4⁺/M-NPs, $n = 5$) and liver transplantation + TLR4⁻/M-NPs group (TLR4⁻/M-NPs, $n = 5$). Rats in the Blank group were not treated. Other groups were treated by injection of 20 mg/kg of corresponding materials into liver transplant recipient rats through the tail vein after successful liver transplantation. The control group was injected with normal saline. Four days later, the liver was removed, and peripheral blood was collected from the rats in each group. Pathological changes in the heart, liver, spleen, lung and kidney were detected by HE staining ($n = 2$). The serum ALT and AST levels were measured at the Experimental Animal Center of Chongqing Medical University ($n = 5$). LPS and inflammatory cytokines, including IL-6 and TNF- α , in the serum were quantified by ELISA as described above ($n = 5$).

Activation of inflammatory pathways in KCs was also used to evaluate the efficacy of M-NPs in neutralizing LPS in an SD rat liver transplantation model. KCs were extracted from rats in each group 4 days later after liver transplantation ($n = 3$). The isolation, purification and identification of KCs from SD rats was performed as

described in our previous study.²¹ LPS-mediated inflammatory-associated proteins, including MyD88, IRAK1, p-p65 and p65, were detected by Western blotting.

Statistical Analyses

All quantitative data are represented as the mean \pm standard error of the mean (SEM). Statistical analyses were performed using SPSS 17.0 software (SPSS, Inc., Chicago, IL, USA). One-way ANOVA with Tukey's post hoc test was used to analyze data sets that included more than two experimental groups, while Student's *t*-test was used to compare data sets based on only two variables. In all analyses, a *p*-value less than 0.05 was considered significant.

Results and Discussion

M-NP Preparation and Characterization

There are three steps involved in preparing macrophage membrane-coated nanoparticles (M-NPs). First, membranes were obtained from RAW264.7 mouse macrophages.^{8,22} Then, poly (lactic-co-glycolic acid) (PLGA) nanoparticles (NPs) were generated according to a previous study.²³ Finally, the macrophage membranes and the NPs were mixed at a mass ratio of 1:2 to prepare M-NPs by repeated extrusion with a liposome extruder (Figure 1A). The morphology and diameters of the NPs and M-NPs were observed by transmission electron microscopy (TEM). The NPs were spherical with a uniform size and diameter of 171.4 ± 17.3 nm (Figure 1B and E). After separation and purification, the macrophage membranes contained transparent fragments (Figure 1C). The M-NPs had a PLGA core wrapped by a transparent shell and a diameter of 214.1 ± 18.6 nm (Figure 1D and E). RAW264.7 macrophages have not only plasma membranes but also nuclear membranes. To investigate the purity of the cell membrane and the coating effect of M-NPs, Western blotting was used to detect the protein expression of the macrophage plasma membrane markers F4/80, TLR4, CD206, and CD11c and the nuclear marker laminA/C in the cell homogenates (Hom), membranes (Mem), nuclei (Nuc) and M-NPs. The isolated membranes only expressed F4/80, TLR4, CD206, and CD11c but not laminA/C, while the cell nuclei only expressed laminA/C but not the plasma membrane markers. This indicates that the separation of the plasma membrane was successful (Figure 1F). In addition, M-NPs only expressed F4/80, TLR4, CD206, and CD11c but not lamin

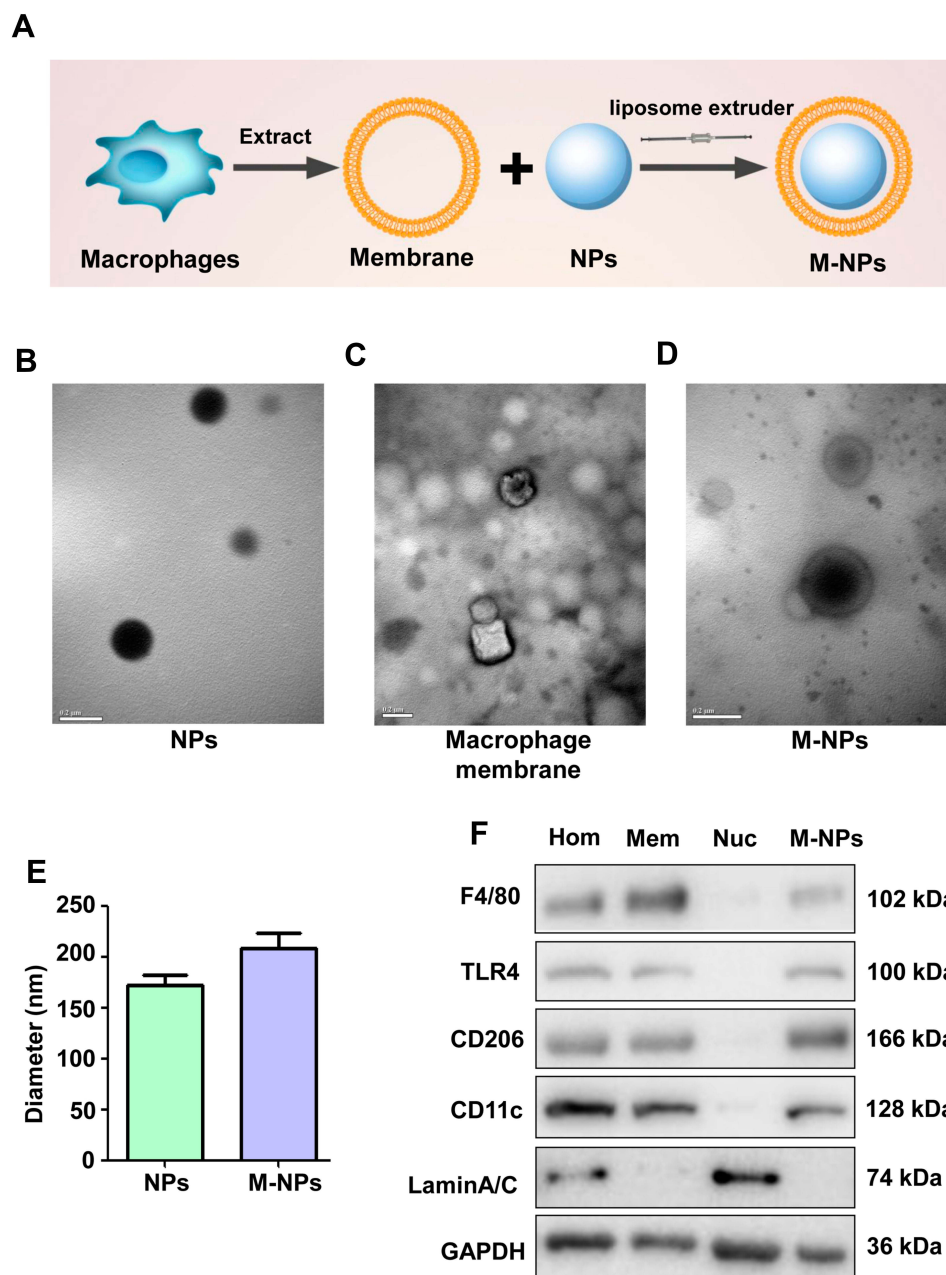


Figure 1 Formulation and characterization of macrophage membrane-coated nanoparticles (M-NPs). Three-step formulation of M-NPs (**A**). TEM images of NPs. (Scale bar: 200 nm) (**B**). TEM images of the macrophage membrane. (Scale bar: 200 nm) (**C**). TEM images of M-NPs. (Scale bar: 200 nm) (**D**). The sizes of the NPs and M-NPs were measured by DLS (**E**). Western blotting was used to detect F4/80, TLR4, CD206, CD11c and lamin A/C protein expression in cell homogenates (Hom), membranes (Mem), nuclei (Nuc) and M-NPs (**F**).

A/C (Figure 1F). Taken together, these results demonstrate the successful generation of M-NPs.

M-NPs Alleviate LPS-Mediated Macrophage Activation

The macrophage membrane contains TLR4, which is an important receptor that triggers the LPS-activated TLR4/MyD88/IRAK1/NF- κ B pathway to induce the inflammatory

response.^{5,24} To examine the ability of M-NPs to bind to LPS and to study the effect of M-NPs on LPS-mediated macrophage activation, we used PLGA nanoparticles as carriers and synthesized M-NPs as previously described. RAW264.7 macrophages in a good growth state were divided into 6 groups, and the macrophages in each group were treated with 150 ng/mL LPS for 24 h. Different concentrations of M-NPs (0, 0.5, 1.0, 2.0, 3.0 and 5.0 mg/mL) were added into

each group of LPS-treated macrophages. Western blotting was used to detect the protein expression of MyD88, IRAK1, p-NF- κ B (p-p65) and NF- κ B (p65). ELISA was used to detect the remaining LPS and the inflammatory factors TNF- α and IL-6 in the supernatant. In the presence of high concentrations of M-NPs, there was decreased protein expression of MyD88, IRAK1 and p-p65 (Figure 2A). Moreover, when the concentration of M-NPs was approximately 2.0 mg/mL, the remaining amount of LPS and the expression of TNF- α and IL-6 in the supernatant were at the lowest levels, indicating that 2.0 mg/mL M-NPs was the optimal concentration for the neutralization of LPS (150 ng/mL) (Figure 2B and C). Subsequently, we further evaluated whether NPs and M-NPs were cytotoxic toward RAW264.7 macrophages. Cell counting kit-8 (CCK-8) assays were used to detect the effect of different concentrations of NPs and M-NPs on macrophage viability in the absence of LPS. We found that when the concentration of NPs or M-NPs exceeded 3.0 mg/mL, NPs or M-NPs significantly inhibited the viability of macrophages ($p < 0.05$) (Figure 2D).

These results showed that M-NPs prepared from bioactive macrophage membranes can effectively inhibit LPS-mediated macrophage activation and reduce the release of

inflammatory factors by neutralizing LPS and inhibiting activation of the TLR4/MyD88/IRAK1/NF- κ B signaling pathway. However, when the concentration of LPS was high, the amount of M-NPs required to neutralize LPS was increased, which increased the risk of the overuse of M-NPs to macrophages. Therefore, we hypothesized that because TLR4 on the macrophage membrane can be overexpressed in vitro, synthesizing TLR4⁺/M-NPs to reduce the amount of M-NPs needed to neutralize an equivalent concentration of LPS would thus reduce the toxic effect of M-NPs on macrophages. To investigate this hypothesis, we silenced or overexpressed TLR4 on macrophage membranes by transfecting TLR4⁻ or TLR4⁺ plasmids and further studied the feasibility of the hypothesis. The plasmid transfection rate was high, and the effect of silencing and overexpressing TLR4 on macrophages after plasmid transfection for 72 h was good (Figure 3A-C). Then, the macrophage membrane-coated nanoparticles were synthesized according to the above described methods to obtain M-NPs, TLR4⁺/M-NPs and TLR4⁻/M-NPs. The experiment was divided into a control group, LPS group, M-NP group, LPS + M-NP group, LPS + TLR4⁺/M-NP group and LPS + TLR4⁻/M-NP group. The control group was not treated. The LPS group was treated with 150 ng/mL LPS for 24

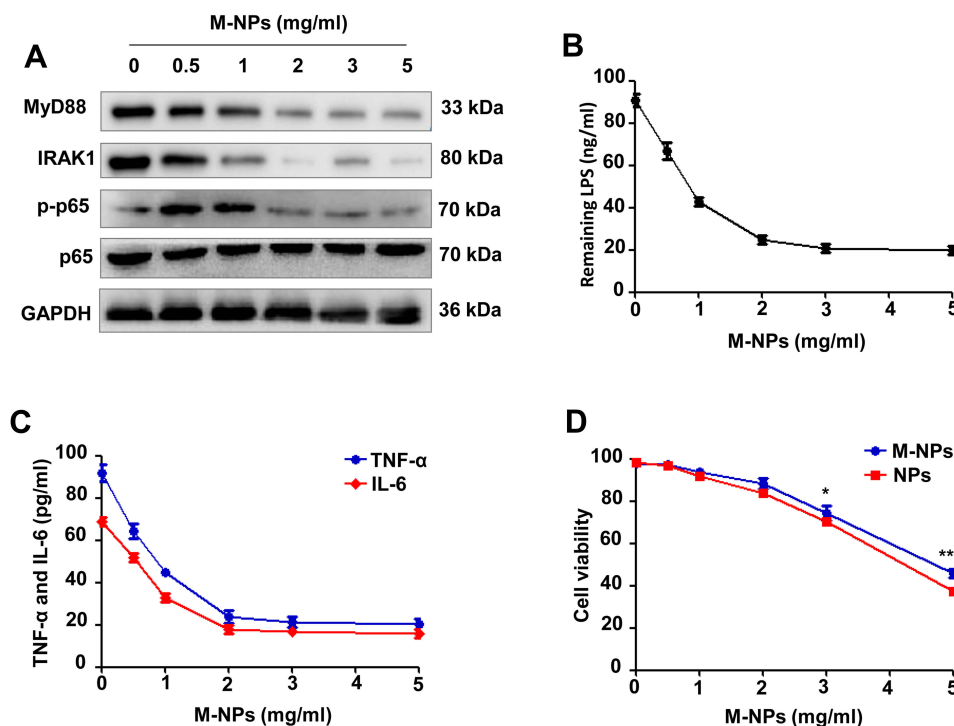


Figure 2 M-NPs alleviate LPS-mediated macrophage activation by neutralizing LPS in vitro. Western blotting was used to detect the protein expression of MyD88, IRAK1, p-p65 and p65 (A). ELISA was used to detect the remaining LPS in the supernatant (B). ELISA was used to detect the levels of TNF- α and IL-6 in the supernatant (C). CCK-8 was used to detect the viability of RAW264.7 macrophages (D). * $p < 0.05$, ** $p < 0.01$.

h. The M-NP group was treated with 1 mg/mL M-NPs for 24 h. The LPS + M-NP group, LPS + TLR4⁺/M-NP group and LPS + TLR4⁻/M-NP group were treated with 150 ng/mL LPS for 24 h, and the corresponding M-NPs at a concentration of 1 mg/mL were added at the same time as the LPS was added. Western blotting was used to detect the expression of the inflammation-related proteins MyD88, IRAK1, p-p65 and p65. Western blotting analysis verified that M-NPs and TLR4⁺/M-NPs both effectively inhibited LPS-induced inflammation-related protein expression in

macrophages (Figure 3D). In addition, quantitative analysis of the remaining LPS in the supernatant of the culture medium showed that the level of LPS in the TLR4⁺/M-NP group was the lowest ($p < 0.05$) (Figure 3E). Moreover, when the concentration of M-NPs or TLR4⁺/M-NPs was less than 3 mg/mL, the consumption of TLR4⁺/M-NPs was less than that of M-NPs when neutralizing the same amount of LPS ($p < 0.05$) (Figure 3F). For example, to neutralize the same LPS concentration as that neutralized by treatment with 3.0 mg/mL M-NPs, the concentration of TLR4⁺/M-NPs

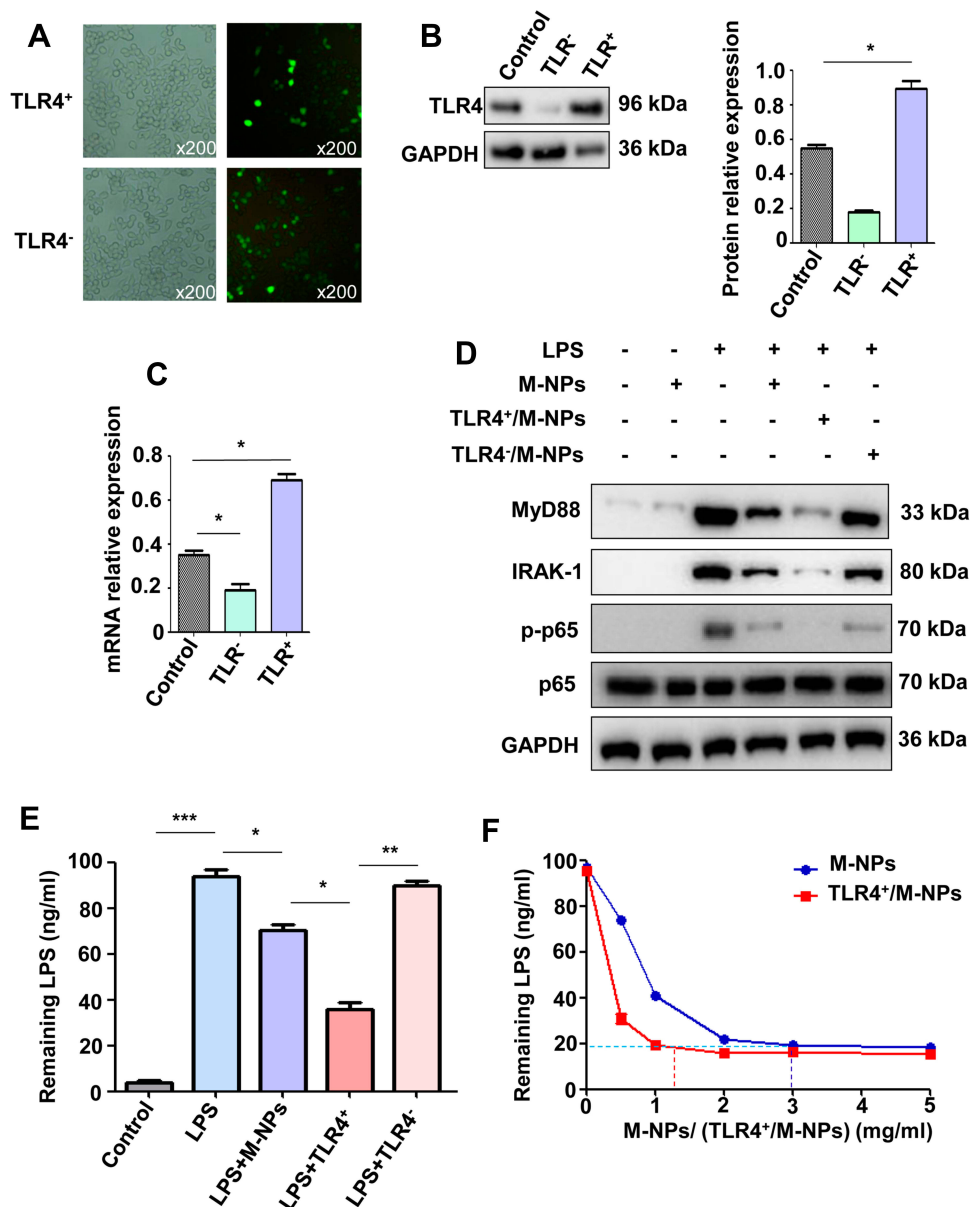


Figure 3 Overexpression of TLR4 on macrophage membranes results in increased inhibition of LPS-mediated macrophage activation. Fluorescence microscopy observations of the transfection efficiency of plasmid transfection for 72 h (Scale bar: x200) (A). Western blotting was used to detect the transfection efficiency (B). qRT-PCR was used to detect the transfection efficiency (C). Western blotting was used to detect the protein expression of MyD88, IRAK1, p-p65 and p65 (D). ELISA was used to detect the remaining LPS in each group (E). ELISA was used to detect the remaining LPS in different concentrations of M-NPs and TLR4⁺/M-NPs (F). * $p < 0.05$, ** $p < 0.01$, *** $p < 0.001$.

required was between 1.0 and 1.5 mg/mL (Figure 3F). As shown in Figure 2D, the toxicity of 1.5 mg/mL M-NPs to macrophages was significantly lower than that of 3.0 mg/mL M-NPs ($p < 0.05$). These results show that in vitro, it is feasible and practical to reduce the NP dose required to neutralize equivalent doses of LPS by overexpressing TLR4 on the macrophage membrane.

M-NPs Alleviate Hepatic I/R in Liver Transplantation

Hepatic I/R is an important cause of liver transplantation failure.²⁵ Hepatic I/R can be divided into ischemic injury and reperfusion injury.²⁶ Gram-negative bacteria produce large amounts of endotoxin that activate KCs and promote the production of inflammatory factors, including IL-6 and TNF- α , which are the main causes of reperfusion injury.²⁷ If endotoxin produced by intestinal G⁻ bacteria can be removed, KC activation will be effectively inhibited, thus reducing hepatic I/R and improving the prognosis of liver transplantation recipients.⁷

Endotoxin is the lipopolysaccharide (LPS) component of the Gram-negative bacterial cell wall. In previous cell experiments, we confirmed that M-NPs effectively inhibited the activation of macrophages and the production of inflammatory factors by neutralizing LPS. We further explored whether M-NPs could be injected into rats after liver transplantation to competitively bind to LPS and reduce the binding of LPS to KCs. Inhibiting the LPS-mediated activation of KCs would inhibit the inflammatory reaction and further inhibit liver transplantation-induced I/R. To explore this hypothesis, we established an SD rat liver transplantation model by the double cuff method, and there was no obvious infection in the wounds of the rats after the operation.²² After successful liver transplantation, we injected the corresponding nanomaterials through the tail vein to explore the effect of M-NPs on rat

liver transplantation and its molecular mechanism. NPs or M-NPs with a red fluorescent probe at a concentration of 15 mg/kg were injected into rats through the tail vein for 24 h. Fluorescence in the rats in the NP and M-NP groups was mainly distributed in the liver, followed by the spleen (Figure 4). This indicated that coating the nanoparticles with the macrophage membranes did not change the distribution of the nanoparticles in the rats.

The experiment was divided into the blank group (Blank), liver transplantation group (control), liver transplantation + NP group (NPs), liver transplantation + M-NP group (M-NPs), liver transplantation + TLR4⁺/M-NP group (TLR4⁺/M-NPs) and liver transplantation + TLR4⁻/M-NP group (TLR4⁻/M-NPs). Rats in the Blank group were not treated. In the other groups, the liver transplant recipient rats were injected with 20 mg/kg NPs or M-NPs through the tail vein after successful liver transplantation. The control group was injected with the same amount of normal saline. Four days later, the liver was removed, and peripheral blood was collected from the rats in each group. Hematoxylin-eosin (HE) staining was used to detect the pathological changes in the heart, liver, spleen, lung and kidney in each group. Liver transplantation significantly exacerbated heart, liver, spleen, lung and kidney injury compared with that observed in the Blank group, which manifested as the destruction of normal tissue structures and the infiltration of inflammatory cells. Injection of NPs alone did not exacerbate or reduce organ damage after liver transplantation (NP group), while M-NPs appropriately reduced the degree of heart, liver, spleen, lung and kidney injury. The degree of heart, liver, spleen, lung and kidney injury in the TLR4⁺/M-NP group was minimal, but TLR4⁻/M-NPs lost their protective effect on the organs (Figure 5A). The results of serum liver function tests were also consistent with the HE

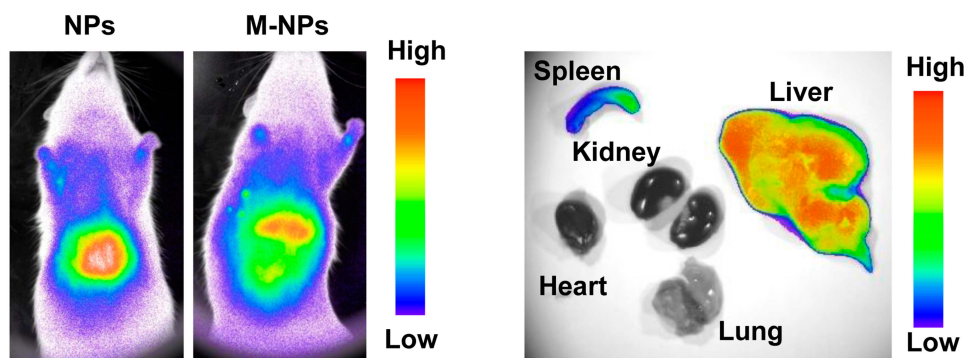


Figure 4 In vivo fluorescence detection of the NP and M-NP distribution in SD rats and organs.

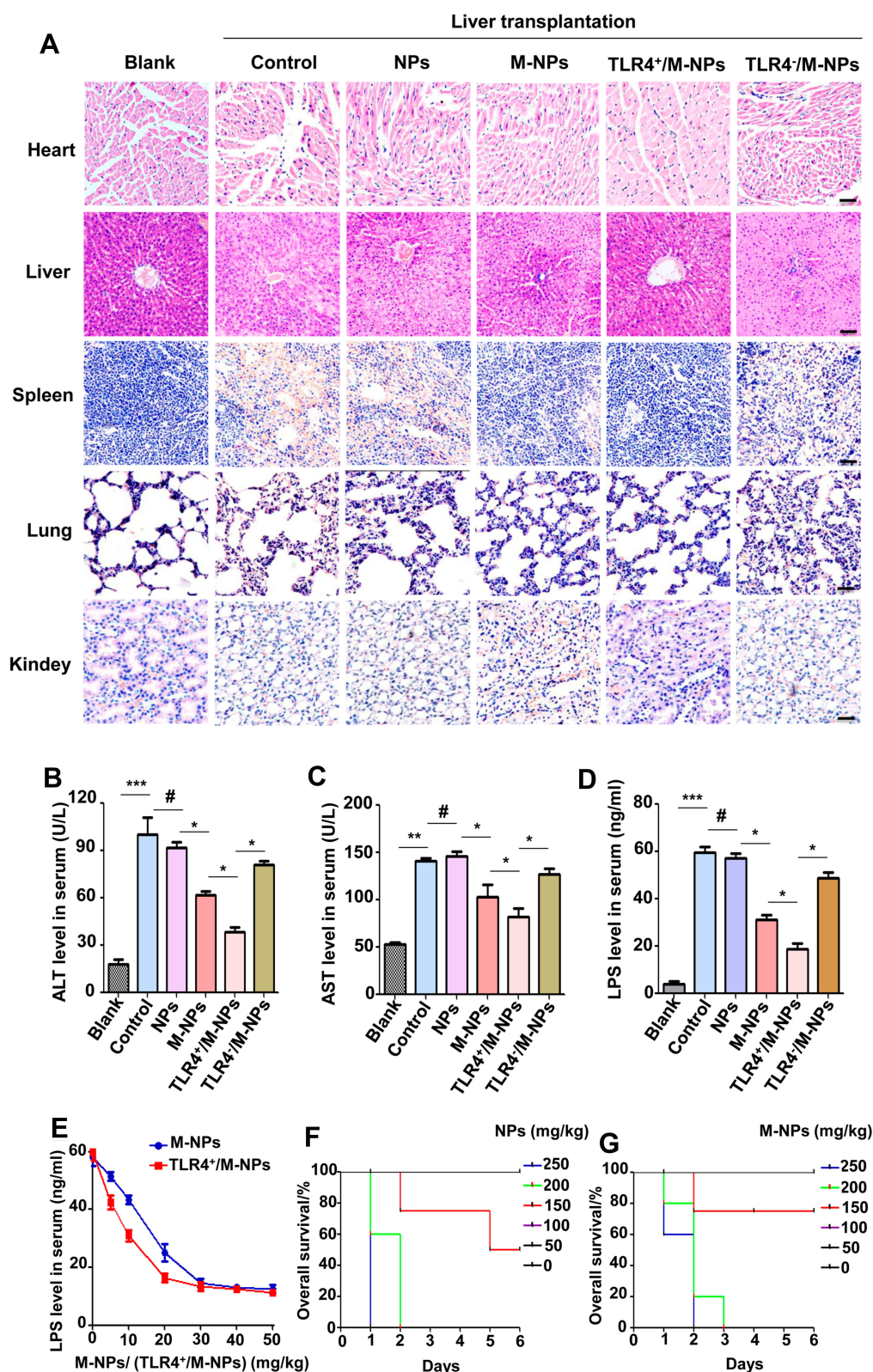


Figure 5 Overexpression of TLR4 on the macrophage membrane reduces liver I/R after liver transplantation. HE staining was used to detect pathological changes in the heart, liver, spleen, lung and kidney. (Scale bar: 1 mm) (A). The level of ALT in serum (B). The level of AST in serum (C). ELISA was used to detect the level of LPS in serum in each group (D). ELISA was used to detect the level of LPS in serum in the presence of different concentrations of M-NPs or TLR4⁺/M-NPs (E). The overall survival of liver transplantation rats treated with different concentrations of NPs (F). The overall survival of liver transplantation rats treated with different concentrations of M-NPs (G). * $p < 0.05$, ** $p < 0.01$, *** $p < 0.001$, # $p > 0.05$.

staining results (Figure 5B and C). That is, injection of NPs alone did not exacerbate or reduce liver function at 4 days after liver transplantation ($p>0.05$). M-NPs improved the liver function of rats after liver transplantation. The rats in the TLR4⁺/M-NP group had better liver function than those in the M-NP group ($p<0.05$). Silencing TLR4 abrogated the protective effect of M-NPs on the liver (Figure 5B and C). We further detected the level of LPS in the serum by ELISA. Liver transplantation significantly increased the LPS content in the serum. The level of LPS in the rats in the M-NP group was lower than that in the control group, and the level of LPS in the TLR4⁺/M-NP group was lower than that in the M-NP group (Figure 5D). These results indicate that M-NPs reduce liver I/R after liver transplantation and that overexpressing macrophage membrane TLR4 in vitro can better protect the liver. Silencing macrophage membrane TLR4 weakens or completely inhibits the protective effect of M-NPs on the liver.

We further studied the correlation between the dose of M-NPs or TLR4⁺/M-NPs and the level of LPS in rat serum. We found that the level of LPS in serum gradually decreased with increasing concentrations of M-NPs or TLR4⁺/M-NPs. In addition, the dose of TLR4⁺/M-NPs required to eliminate the same amount of LPS (Figure 5E) was less than that of M-NPs. To reduce LPS in rat serum to the lowest level, the concentration of M-NPs needed was approximately 30 mg/kg, while the

concentration of TLR4⁺/M-NPs needed was approximately 20 mg/kg (Figure 5E). We further studied the effect of NP/M-NP concentrations on toxicity in liver transplantation rats. We found that when the concentration of NPs or M-NPs exceeded 250 mg/kg in a rat after liver transplantation, the rat ($n = 5$) died within 2 days (Figure 5F and G). The exact cause of death was unknown and may be associated with acute liver failure. However, this indicates that excessive use of nanomaterials poses serious risks to liver transplantation rats. Further studies confirmed that concentrations of NPs or M-NPs less than 100 mg/kg in each rat were relatively safe (Figure 5F and G). Although the concentration of M-NPs or TLR4⁺/M-NPs did not exceed 100 mg/kg (damage threshold for rats) when the LPS in serum was reduced to the lowest level, the above described results highlight the importance of reducing the dose of nanomaterials. Here, by overexpressing macrophage membrane TLR4 in vitro and preparing TLR4⁺/M-NPs, the dose of TLR4⁺/M-NPs needed to reduce the same amount of LPS in the serum of rats after liver transplantation was significantly lower than the corresponding dose of M-NPs. Reducing the dose of nanomaterials is a method to reduce the potential risks of using nanomaterials.

KCs are macrophages located in the hepatic sinusoid that account for 80~90% of the total macrophages in the body, and they play an important role in regulating the immune response of the body.¹³ Studies have shown that

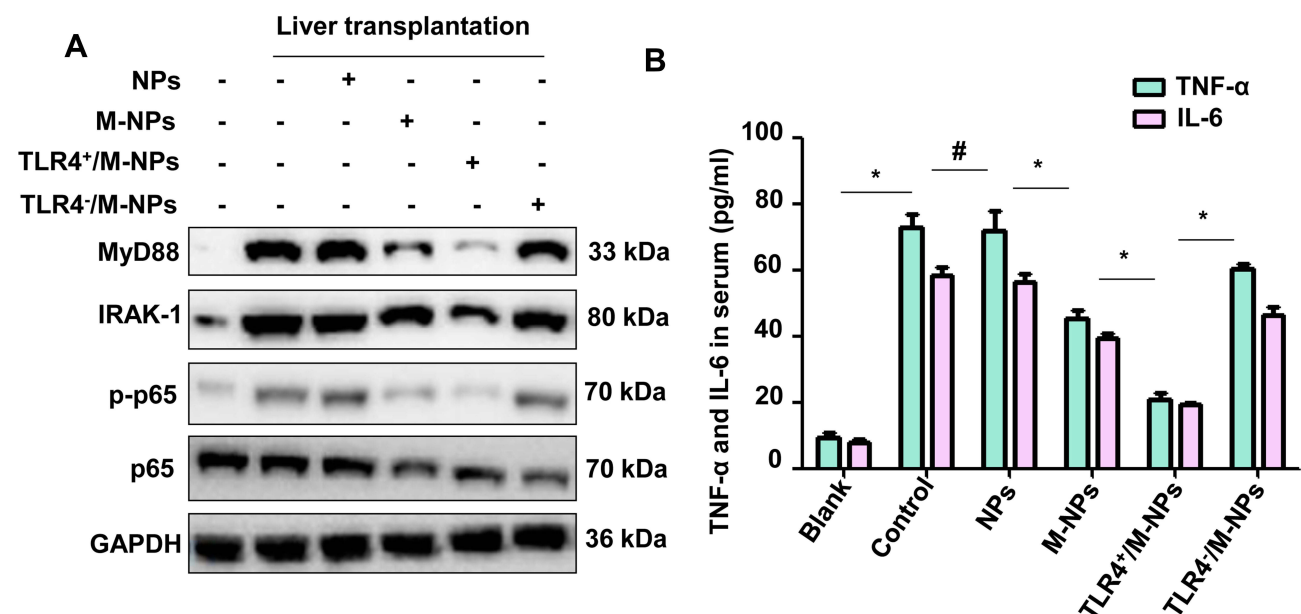


Figure 6 M-NPs relieve liver I/R by neutralizing LPS, inhibiting activation of the inflammatory pathway in KCs and inhibiting the expression of inflammatory factors. Western blotting was used to detect the protein expression of MyD88, IRAK1, p-p65 and p65 (A). ELISA was used to detect the levels of TNF-α and IL-6 in the serum of each group (B). * $p < 0.05$, # $p > 0.05$.

inhibiting KC activation during liver transplantation effectively improves the efficacy of liver transplantation and improves the prognosis of liver transplantation recipients.^{7,20} Therefore, we isolated KCs from SD rats through our previously described methods and investigated the activation of KCs in rats in each group to further study the molecular mechanism by which M-NPs alleviate hepatic I/RI after liver transplantation.²¹ Western blotting was used to detect the expression of the inflammation-related proteins MyD88, IRAK1, p-p65 and p65. Western blotting analysis showed that liver transplantation activated the inflammatory pathway in KCs, and M-NP injection effectively inhibited activation of the inflammatory pathway in KCs and inhibited the expression of the inflammatory factors TNF- α and IL-6. TLR4⁺/M-NP injection more effectively inhibited the activation of the KC inflammatory pathway and the level of inflammatory factors in serum compared with M-NP injection (Figure 6A and B). These results show that M-NPs relieved liver I/RI in liver

transplantation by neutralizing LPS. In addition, when the same amount of LPS was neutralized with M-NPs or TLR4⁺/M-NPs, the dose of TLR4⁺/M-NPs needed was significantly less than that of M-NPs, which greatly reduced the potential harm of NPs to the body.

Conclusions

In summary, we explored the effect of macrophage membrane-coated nanoparticles (M-NPs) on hepatic I/RI after rat liver transplantation and the molecular mechanism (Figure 7). In vitro, M-NPs effectively inhibited LPS-mediated activation of RAW264.7 macrophages. In vivo, M-NPs alleviated liver transplantation-induced liver dysfunction and multiple organ injury in rats by neutralizing LPS and suppressing the LPS-mediated activation of KCs by inhibiting the TLR4/MyD88/IRAK1/NF- κ B signaling pathway. Moreover, we found that excessive use of nanomaterials has various toxic effects on RAW264.7 macrophages and rats after liver transplantation. Therefore, for the first time,

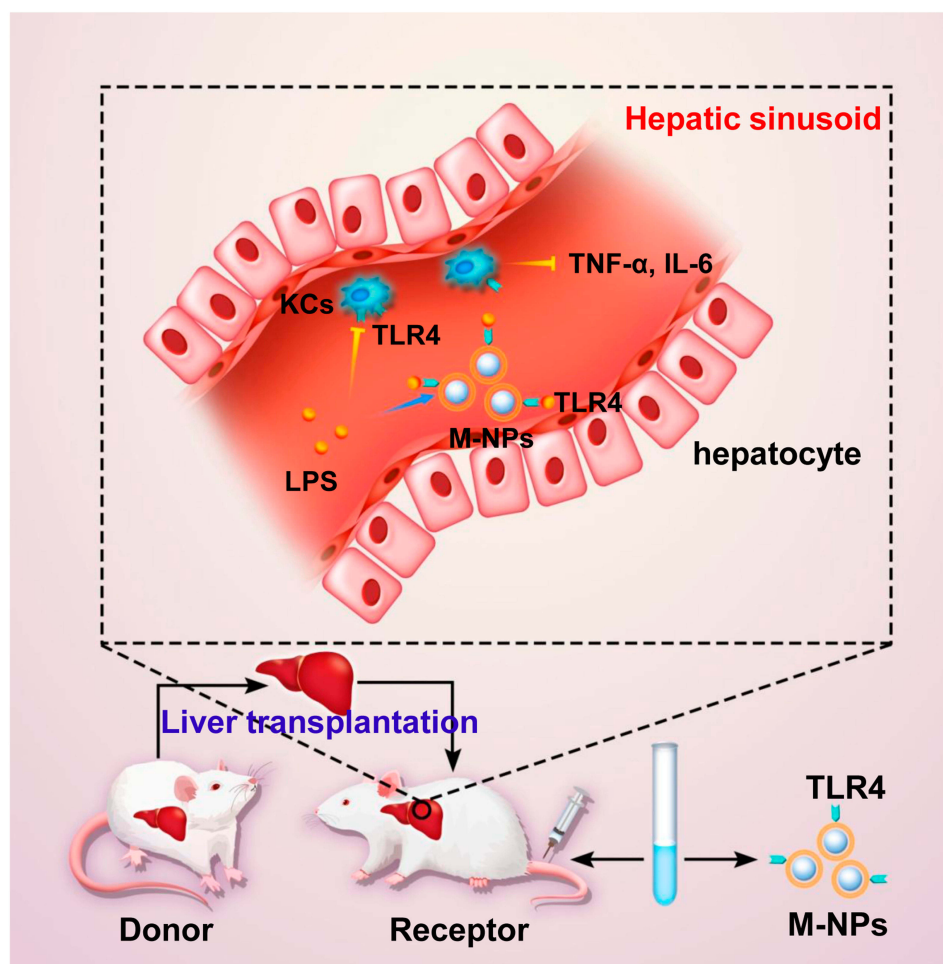


Figure 7 Schematic representation of the proposed underlying mechanism of the alleviation of hepatic I/RI caused by liver transplantation by M-NPs.

we silenced or overexpressed TLR4 on macrophage membranes by transfecting TLR4⁻ or TLR4⁺ plasmids. Overexpressing TLR4 on the macrophage membrane in vitro increases the amount of TLR4 per unit of the macrophage membrane area. TLR4⁺/M-NPs synthesized by this method had more LPS binding sites than ordinary M-NPs, thus reducing the amount of NPs needed to neutralize the same dose of LPS, which reduced the potential risks of NP overuse. This method provides a reference for other similar studies and has certain theoretical and practical significance.

Acknowledgments

This work was supported by the National Natural Science Foundation of China (No. 81701957), the Natural Science Foundation of Chongqing (cstc2019jcyj-msxmX0620), China Postdoctoral Science Foundation (2019M653352) and Scientific Research Projects of Chenzhou No.1 People's Hospital (BSQDJ-020). The study was approved by the Research Ethics Committee of Chongqing Medical University (2019-107).

Author Contributions

All authors contributed to data analysis, drafting and revising the article, gave final approval of the version to be published, and agree to be accountable for all aspects of the work.

Disclosure

The authors report no conflicts of interest in this work.

References

- Forbes SJ, Gupta S, Dhawan A. Cell therapy for liver disease: from liver transplantation to cell factory. *J Hepatol*. 2015;62(1):S157–169. doi:10.1016/j.jhep.2015.02.040
- Dienstag JL, Cosimi AB. Liver transplantation—a vision realized. *N Engl J Med*. 2012;367(16):1483–1485. doi:10.1056/NEJMp1210159
- Dar WA, Sullivan E, Bynon JS, et al. Ischaemia reperfusion injury in liver transplantation: cellular and molecular mechanisms. *Liver Int*. 2019;39(5):788–801. doi:10.1111/liv.14091
- Huang H, Lu Y, Zhou T, et al. Innate immune cells in immune tolerance after liver transplantation. *Front Immunol*. 2018;9:2401. doi:10.3389/fimmu.2018.02401
- Li P, He K, Li J, et al. The role of Kupffer cells in hepatic diseases. *Mol Immunol*. 2017;85:222–229. doi:10.1016/j.molimm.2017.02.018
- Golden-Mason L, Rosen HR. Galectin-9: diverse roles in hepatic immune homeostasis and inflammation. *Hepatology*. 2017;66(1):271–279. doi:10.1002/hep.29106
- Marshall K, Jin J, Atkinson C, et al. Natural immunoglobulin M initiates an inflammatory response important for both hepatic ischemia reperfusion injury and regeneration in mice. *Hepatology*. 2018;67(2):721–735. doi:10.1002/hep.29512
- Fang RH, Hu C-MJ, Luk BT, et al. Cancer cell membrane-coated nanoparticles for anticancer vaccination and drug delivery. *Nano Lett*. 2014;14(4):2181–2188. doi:10.1021/nl500618u
- Narain A, Asawa S, Chhabria V, et al. Cell membrane coated nanoparticles: next-generation therapeutics. *Nanomedicine (Lond)*. 2017;12(21):2677–2692. doi:10.2217/nnm-2017-0225
- Zhang Q, Dehaini D, Zhang Y, et al. Neutrophil membrane-coated nanoparticles inhibit synovial inflammation and alleviate joint damage in inflammatory arthritis. *Nat Nanotechnol*. 2018;13(12):1182–1190. doi:10.1038/s41565-018-0254-4
- Hu CM, Fang RH, Wang K-C. Nanoparticle biointerfacing by platelet membrane cloaking. *Nature*. 2015;526(7571):118–121. doi:10.1038/nature15373
- Escajadillo T, Olson J, Luk BT, et al. Red blood cell membrane-camouflaged nanoparticle counteracts streptolysin o-mediated virulence phenotypes of invasive group A streptococcus. *Front Pharmacol*. 2017;8:477. doi:10.3389/fphar.2017.00477
- Tacke F. Targeting hepatic macrophages to treat liver diseases. *J Hepatol*. 2017;66(6):1300–1312. doi:10.1016/j.jhep.2017.02.026
- Liu Q, Wang X, Liu X, et al. Use of polymeric nanoparticle platform targeting the liver to induce treg-mediated antigen-specific immune tolerance in a pulmonary allergen sensitization model. *ACS Nano*. 2019;13(4):4778–4794. doi:10.1021/acsnano.9b01444
- Lu YC, Yeh WC, Ohashi PS. LPS/TLR4 signal transduction pathway. *Cytokine*. 2008;42(2):145–151. doi:10.1016/j.cyto.2008.01.006
- Li J, Zhen X, Lyu Y, et al. Cell membrane coated semiconducting polymer nanoparticles for enhanced multimodal cancer phototheranostics. *ACS Nano*. 2018;12:8520–8530. doi:10.1021/acsnano.8b04066
- Tan ST, Liu SY, Wu B. TRIM29 overexpression promotes proliferation and survival of bladder cancer cells through NF-κB signaling. *Cancer Res Treat*. 2016;48(4):1302–1312. doi:10.4143/crt.2015.381
- Toledo M, Batista-Gonzalez A, Merheb E, et al. Autophagy regulates the liver clock and glucose metabolism by degrading CRY1. *Cell Metab*. 2018;28(2):268–281. doi:10.1016/j.cmet.2018.05.023
- Chen X, Wang L, Deng Y, et al. Inhibition of autophagy prolongs recipient survival through promoting CD8⁺ T cell apoptosis in a rat liver transplantation model. *Front Immunol*. 2019;10:1356. doi:10.3389/fimmu.2019.01356
- Zhao Z, Pan G, Tang C, et al. IL-34 inhibits acute rejection of rat liver transplantation by inducing Kupffer cell M2 polarization. *Transplantation*. 2018;102(6):e265–e274. doi:10.1097/TP.0000000000002194
- Zeng WQ, Zhang JQ, Li Y, et al. A new method to isolate and culture rat kupffer cells. *PLoS One*. 2013;8(8):e70832. doi:10.1371/journal.pone.0070832
- Thamphiwatana S, Angsantikul P, Escajadillo T, et al. Macrophage-like nanoparticles concurrently absorbing endotoxins and proinflammatory cytokines for sepsis management. *Proc Natl Acad Sci U S A*. 2017;114(43):11488–11493. doi:10.1073/pnas.1714267114
- Wang Y, Zhang K, Qin X, et al. Biomimetic nanotherapies: red blood cell based core-shell structured nanocomplexes for atherosclerosis management. *Adv Sci (Weinh)*. 2019;6(12):1900172. doi:10.1002/advs.201900172
- Liu B, Zheng Y, Yin F, et al. Toll receptor-mediated hippo signaling controls innate immunity in Drosophila. *Cell*. 2016;164(3):406–419. doi:10.1016/j.cell.2015.12.029
- Trapero-Marugán M, Little EC, Berenguer M. Stretching the boundaries for liver transplant in the 21st century. *Lancet Gastroenterol Hepatol*. 2018;3(11):803–811. doi:10.1016/S2468-1253(18)30213-9
- Xu J, Xue Z, Zhang C, et al. Inhibition of Cyclin-dependent Kinase 2 signaling prevents liver ischemia and reperfusion injury. *Transplantation*. 2019;103(4):724–732. doi:10.1097/TP.0000000000002614
- Shi S, Verstegen MMA, Mezzanotte L, et al. Necroptotic cell death in liver transplantation and underlying diseases: mechanisms and clinical perspective. *Liver Transpl*. 2019;25(7):1091–1104. doi:10.1002/lt.25488

International Journal of Nanomedicine**Dovepress****Publish your work in this journal**

The International Journal of Nanomedicine is an international, peer-reviewed journal focusing on the application of nanotechnology in diagnostics, therapeutics, and drug delivery systems throughout the biomedical field. This journal is indexed on PubMed Central, MedLine, CAS, SciSearch®, Current Contents®/Clinical Medicine,

Journal Citation Reports/Science Edition, EMBase, Scopus and the Elsevier Bibliographic databases. The manuscript management system is completely online and includes a very quick and fair peer-review system, which is all easy to use. Visit <http://www.dovepress.com/testimonials.php> to read real quotes from published authors.

Submit your manuscript here: <https://www.dovepress.com/international-journal-of-nanomedicine-journal>